



# Immunity to commensal skin fungi promotes psoriasiform skin inflammation

Charlotte Hurabielle<sup>a,b,c,1</sup>, Verena M. Link<sup>a,1</sup>, Nicolas Bouladoux<sup>a,d</sup>, Seong-Ji Han<sup>a</sup>, Eric Dean Merrill<sup>a,e</sup>, Yaima L. Lightfoot<sup>f,g</sup>, Nickie Seto<sup>f</sup>, Christopher K. E. Bleck<sup>h</sup>, Margery Smelkinson<sup>i</sup>, Oliver J. Harrison<sup>a,j</sup>, Jonathan L. Linehan<sup>a,k</sup>, Samira Tamoutounour<sup>a,2</sup>, Michail S. Lionakis<sup>l</sup>, Mariana J. Kaplan<sup>f</sup>, Saeko Nakajima<sup>a,m,3</sup>, and Yasmine Belkaid<sup>a,d,3</sup>

<sup>a</sup>Metaorganism Immunity Section, Laboratory of Immune System Biology, National Institute of Allergy and Infectious Diseases, NIH, Bethesda, MD 20892; <sup>b</sup>Inserm Unit 976, Hôpital Saint-Louis, 75010 Paris, France; <sup>c</sup>San Francisco Internal Medicine, University of California, San Francisco, CA 94143; <sup>d</sup>Microbiome Program, National Institute of Allergy and Infectious Diseases, NIH Bethesda, MD 20892; <sup>e</sup>San Francisco Dermatology, University of California, San Francisco, CA 94115; <sup>f</sup>Systemic Autoimmunity Branch, National Institute of Arthritis and Musculoskeletal and Skin Diseases, NIH, Bethesda, MD 20892; <sup>g</sup>Neurodegeneration Consortium, University of Texas MD Anderson Cancer Center, Houston, TX 77054; <sup>h</sup>Electron Microscopy Core Facility, National Heart, Lung, and Blood Institute, NIH, Bethesda, MD 20892; <sup>i</sup>Biological Imaging, Research Technology Branch, National Institute of Allergy and Infectious Diseases, NIH, Bethesda, MD 20892; <sup>j</sup>Immunology Program, Benaroya Research Institute, Seattle, WA 98101; <sup>k</sup>Department of Cancer Immunology, Genentech, South San Francisco, CA 94080; <sup>l</sup>Fungal Pathogenesis Section, Laboratory of Clinical Immunology and Microbiology, National Institute of Allergy and Infectious Diseases, NIH, Bethesda, MD 20892; and <sup>m</sup>Department of Dermatology, Kyoto University Graduate School of Medicine, Sakyo, 606-8507 Kyoto, Japan

Contributed by Yasmine Belkaid, May 17, 2020 (sent for review February 24, 2020; reviewed by Daniel Kaplan and Esther von Stebut-Borschitz)

**Under steady-state conditions, the immune system is poised to sense and respond to the microbiota. As such, immunity to the microbiota, including T cell responses, is expected to precede any inflammatory trigger. How this pool of preformed microbiota-specific T cells contributes to tissue pathologies remains unclear. Here, using an experimental model of psoriasis, we show that recall responses to commensal skin fungi can significantly aggravate tissue inflammation. Enhanced pathology caused by fungi preexposure depends on Th17 responses and neutrophil extracellular traps and recapitulates features of the transcriptional landscape of human lesional psoriatic skin. Together, our results propose that recall responses directed to skin fungi can directly promote skin inflammation and that exploration of tissue inflammation should be assessed in the context of recall responses to the microbiota.**

skin | psoriasis | fungi | microbiota | Th17

Tissues exposed to the environment are primary sites of exposure to symbiotic microbes. These microbes not only contribute to the development and function of the immune system but are also continuously sensed by the immune system (1). The result of this dialogue is the induction of cognate, non-inflammatory B and T cell responses that control various aspects of tissue function (2–5). The contribution of this pool of preformed microbiota-reactive T cells to the etiology of inflammatory disorders and particularly to those occurring in tissues colonized by the microbiota remains unclear.

Previous work revealed that the homeostatic dialogue between the host and its microbiota can be threatened in the context of inflammatory disorders, defined genetic predispositions, or infections (6–8). For instance, in humans, aberrant reactivity to the microbiota has been documented in the context of several diseases including inflammatory bowel disease and, in mice, immune responses to defined members of the gut microbiota can enhance both local and systemic inflammatory responses (9, 10). However, in most settings, it remains unclear to which extent aberrant immunity to the microbiota occurs as a bystander of inflammatory processes as opposed to as a driver and/or amplifier of disease states.

As for all barrier sites, the skin is tightly controlled by its resident microbes (11). These microbes promote the induction of homeostatic immune responses dominated by the accumulation of IL-17A-producing T cells (11–13). While IL-17A can promote tissue homeostasis and antimicrobial defense (14), this cytokine is also a major player in the etiology of skin inflammatory disorders including psoriasis (15, 16). Psoriatic flares have been

associated with skin microbiota alterations (17–19) and experimental evidence supports a role for the microbiota in the etiology of this disorder (20, 21). However, psoriasis is not associated with a defined microbial signature supporting the idea that canonical microbes able to engage type-17 responses, rather than specific members of the microbiota, may contribute to the induction and/or amplification of this inflammatory disorder (22).

Fungi are potent inducers of type-17 polarized responses, a class of immunity that is fundamental to their containment (23). Skin fungi are also constitutive members of the skin microbiome (24, 25). While recent evidence linked this class of microbes to

## Significance

Tissues exposed to the environment are sites of exposure to symbiotic microbes including fungi that are continuously sensed by the immune system. Here, we show that immunity to commensal skin fungi can significantly aggravate tissue inflammation. Enhanced pathology caused by fungi preexposure depends on lymphocytes able to produce the cytokine IL-17 and the formation of extracellular traps by neutrophils. We also found that fungal exposure prior to experimental modeling of psoriasis recapitulates features of the transcriptional landscape of human lesional psoriatic skin. Together, our results propose that recall responses directed to skin fungi can directly promote skin inflammation and that exploration of tissue inflammation should be assessed in the context of recall responses to the microbiota.

Author contributions: C.H., V.M.L., S.N., and Y.B. designed research; C.H., V.M.L., N.B., S.-J.H., E.D.M., Y.L.L., N.S., C.K.E.B., M.S., O.J.H., J.L.L., S.T., and S.N. performed research; M.S.L. and M.J.K. contributed new reagents/analytic tools; C.H., V.M.L., N.B., S.-J.H., E.D.M., Y.L.L., N.S., C.K.E.B., M.S., O.J.H., S.T., and S.N. analyzed data; and C.H., V.M.L., S.N., and Y.B. wrote the paper.

Reviewers: D.K., University of Pittsburgh; and E.V.S.-B., University of Cologne.

Competing interest statement: D.K. and S.N. are coauthors on a 2012 original article and a 2018 review paper. S.T. is an employee of L'Oréal Research and Innovation.

Published under the PNAS license.

Data deposition: The RNA-seq datasets were deposited with the National Center for Biotechnology Information (NCBI) under accession no. GSE144850.

<sup>1</sup>C.H. and V.M.L. contributed equally to this work.

<sup>2</sup>Present address: L'Oréal Advanced Research, L'Oréal Research and Innovation, 93600 Aulnay-sous-Bois, France.

<sup>3</sup>To whom correspondence may be addressed. Email: fujiko@kuhp.kyoto-u.ac.jp or ybelkaid@niaid.nih.gov.

This article contains supporting information online at <https://www.pnas.org/lookup/suppl/doi:10.1073/pnas.2003022117/-DCSupplemental>.

First published June 29, 2020.

the control of gut and lung immunity (26), a role for commensal fungi in skin homeostasis and disease etiologies remains unclear. In support of a potential link between the fungal microbiome and disease etiology, lesional skin of psoriasis patients is characterized by an altered fungal microbiome compared to healthy controls (27–32). Further, characterization of the skin fungal flora of psoriatic patients also revealed an enrichment in *Candida* species (27–33) and defined psoriatic patients can positively respond to antifungals (34). Of particular interest, a large fraction of circulating Th17 clones in humans have been shown to be reactive to fungal antigens and in particular are specific for *Candida albicans* (35) and a recent study revealed that, in humans, fungi-specific Th17 cells can cross-react to antigens expressed by diverse fungi and expand in patients with airway inflammation (36).

In the present study, we hypothesized that preexisting type-17 immunity to canonical fungal microbes could contribute to the etiology of skin inflammatory disorders. Our results reveal that mobilization of preformed fungal-specific T cells to inflammatory sites can significantly aggravate tissue pathology in a Th17-dependent and neutrophil extracellular traps-dependent manner. Further, fungal preexposure prior to treatment with imiquimod (IMQ) recapitulates the transcriptional landscape of human lesional psoriatic skin more closely than the well-established model of imiquimod-induced psoriasis. Together, these results propose that recall responses directed to skin fungi can directly promote skin inflammation and provide a model of experimental psoriasis with translational relevance.

## Results

**Fungal Skin Colonization Drives a Polarized IL-17A<sup>+</sup> T Cell Response and Exacerbates Psoriasis-like Skin Inflammation.** How commensal fungi are sensed by the skin immune system under steady-state conditions has not been addressed. Using our previously described model of skin association (3), we topically applied skin fungi including *C. albicans*, *Malassezia furfur*, and *Trichophyton mentagrophytes*. As we previously showed for bacterial commensals (3, 37) topical application of commensal fungi was not associated with tissue inflammation as evidenced by a lack of skin thickening, inflammatory cell recruitment, erythema, or hyperkeratosis (SI Appendix, Fig. S1 B–D). Despite the lack of inflammation, *C. albicans* and *M. furfur* enhanced CD4<sup>+</sup> T cells recruitment within the skin and the three fungi promoted the accumulation of IL-17A-producing CD4<sup>+</sup> T cells (Th17) (Fig. 1 A and B and SI Appendix, Fig. S1E). *C. albicans* and *M. furfur* also induced a significant increase of CD8<sup>+</sup> T cells within the skin with enhanced accumulation of IL-17A-producing CD8<sup>+</sup> T cells (Tc17) for the three fungi tested (Fig. 1A). *M. furfur* also promoted a significant accumulation of IL-17A-producing  $\gamma\delta$  T cells within the skin compartment (Fig. 1A). This was in contrast to intradermal injection of *C. albicans*, which led to strong skin inflammation and mixed polarized responses dominated by Th1 (SI Appendix, Fig. S1F). Thus, cutaneous colonization with commensal skin fungi is associated with the induction of highly polarized non-inflammatory type-17 skin immune responses.

Based on the clinical association between IL-17A and psoriasis etiology (38), we next assessed to which extent the preexistence of commensal fungi-induced type-17 responses could impact skin inflammation. To this end, we utilized the experimental model of psoriasis associated with the topical application of IMQ, a TLR7 (and TLR8 in humans) agonist. This regimen promotes a psoriasis-like skin inflammation, mediated by the IL-23/IL-17 axis (39, 40). Using this model, we found that preexposure to each of the skin fungi significantly exacerbated skin inflammatory response to IMQ compared to IMQ alone (Fig. 1C).

To gain mechanistic insights into the enhanced pathology associated with fungi preexposure, we next focused on *C. albicans* because of its genetic tractability. Following *C. albicans* association, fungi stably colonize the skin and are maintained at low

colony forming units (CFUs) for months postassociation (SI Appendix, Fig. S1A). Increased pathology in mice associated with *C. albicans* prior to IMQ treatment was characterized by enhanced hyperplastic epidermis, acanthosis, spongiosis, hyperkeratosis, and enhanced inflammatory infiltrate compared to IMQ treatment alone and was not associated with significant changes in skin fungal load (Fig. 1D and SI Appendix, Fig. S1 A and G). On the other hand, the frequencies and absolute numbers of type-17 (IL-17A- and ROR $\gamma$ t-expressing) CD4<sup>+</sup> (but not T<sub>reg</sub>) cells were significantly increased in mice exposed to *C. albicans* before IMQ treatment compared to all of the other groups (Fig. 1 E and F and SI Appendix, Fig. S1H). Increase in Th17 cell accumulation and enhanced IMQ-induced pathology were observed with several strains of *C. albicans* (SI Appendix, Fig. S1I) and persisted for at least up to 2 mo postinitial colonization (Fig. 1G).

We next assessed if the impact of *C. albicans* was direct or dependent on *C. albicans*-induced alteration in the endogenous microbial community. As previously shown, mice raised in absence of live microbes (germ free [GF]) have reduced numbers of IL-17A-producing T cells within the skin (3). *C. albicans* association prior to treatment with IMQ significantly enhanced tissue inflammation and Th17 cell responses as compared to IMQ treatment alone in GF mice (Fig. 1H). Thus, the impact of *C. albicans* on IMQ-induced inflammation can occur in the absence of other skin microbes.

While *C. albicans* is a normal constituent of the microbiome (41), this microbe can also cause active infection. As such, we next assessed if the impact of *C. albicans* on IMQ-induced inflammation resulted from an active infection caused by barrier disruption or from skin colonization. *C. albicans* is a dimorphic fungus, with a yeast form able to colonize the stratum corneum, and a pathogenic hyphal form able to invade the dermis and systemic organs (42). Periodic acid Schiff (PAS) staining revealed that *C. albicans* remained in its yeast form localized on the stratum corneum in the context of IMQ-induced inflammation (SI Appendix, Fig. S1J). Further, a yeast-locked *hgc1Δ* strain of *C. albicans*, which cannot make the transition from the yeast to the hyphal form (43), was also able to exacerbate IMQ-induced psoriasis-like dermatitis (Fig. 1I). Thus, *C. albicans* exacerbated IMQ-induced skin inflammation was not associated with active infection but resulted from skin colonization.

**Enhanced Pathology Caused by Fungal Preexposure Recapitulates the Transcriptional Landscape of Human Lesional Psoriatic Skin.** To compare tissue responses to *C. albicans*, *C. albicans* prior to IMQ, and IMQ alone, we performed whole-tissue RNA sequencing (RNA-seq) in biological replicates (SI Appendix, Fig. S2A). No differences were observed in gene expression from naive control versus *C. albicans*-associated skin confirming that *C. albicans* association alone was noninflammatory (Figs. 1D and 2A and SI Appendix, Fig. S2B).

On the other hand and as previously described (40), IMQ treatment had a profound impact on the skin transcriptional profile, with about 1,500 genes differentially expressed between naive tissue and tissue treated with IMQ (fold change [FC] > 2, false discovery rate [FDR] < 5%) (SI Appendix, Fig. S2C). Association with *C. albicans* prior to IMQ treatment induced a more pronounced change in gene expression with about 3,000 genes differentially expressed between naive and *C. albicans*/IMQ-treated skin (FC > 2, FDR < 5%) (SI Appendix, Fig. S2 D and E).

In order to gain insights into potential pathways associated with enhanced pathology in *C. albicans*/IMQ as compared to IMQ alone, we performed gene ontology (GO) enrichment analysis. Both treatments showed similar enrichment of functional annotations as compared to naive control tissue with cell cycle being the most enriched term followed by inflammatory response, keratinization, neutrophil migration/degranulation,

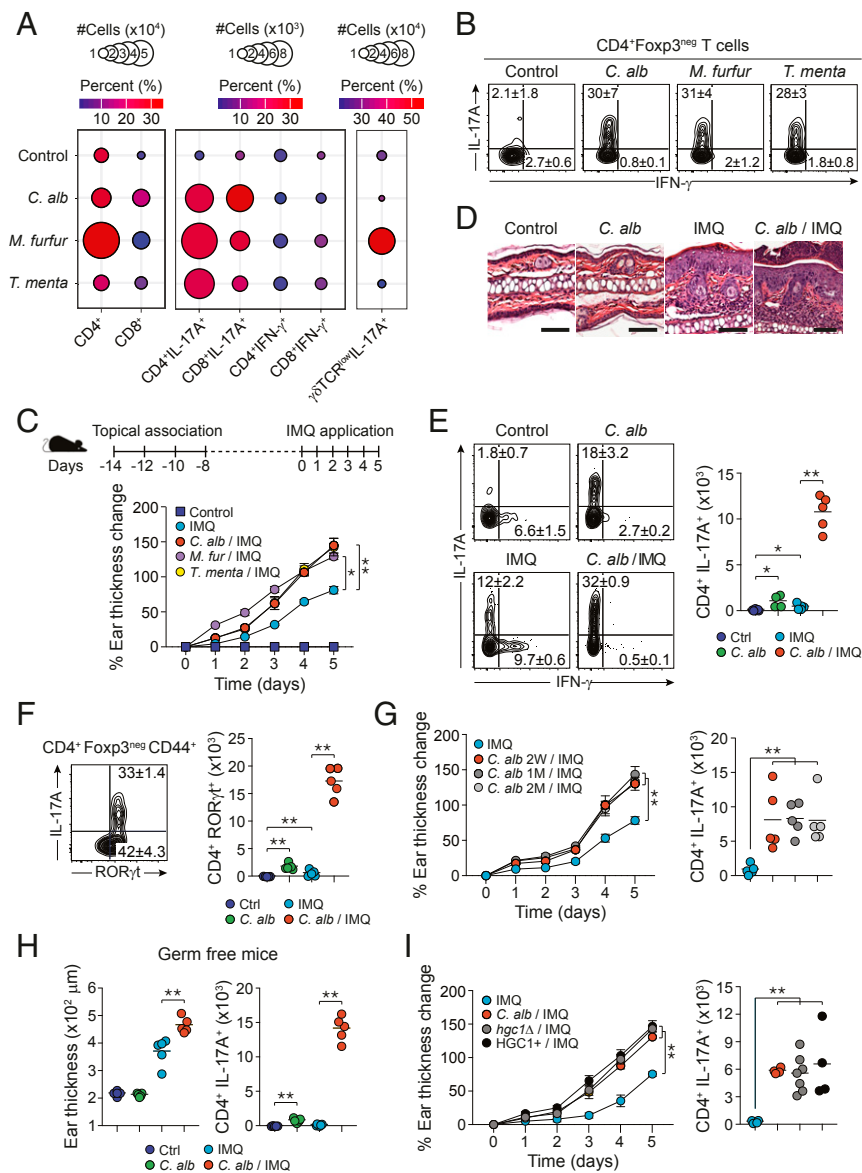


**Fig. 1.** Skin-colonized *C. albicans* exacerbates the inflammation of psoriasis-like dermatitis. (A and B) SPF mice were topically associated with media (control) or various commensal fungi four times every other day: *C. albicans* (*C. alb*), *M. furfur* (*M. furfur*), and *T. mentagrophytes* (*T. menta*). (A) Mean of absolute numbers (represented by the size of the circles) and frequencies (represented by the color of the circles) of live CD45<sup>+</sup>CD90.2<sup>+</sup>TCR $\beta$ <sup>+</sup>Foxp3<sup>neg</sup>CD4<sup>+</sup> (CD4<sup>+</sup>) and CD45<sup>+</sup>CD90.2<sup>+</sup>TCR $\beta$ <sup>+</sup>Foxp3<sup>neg</sup>CD8<sup>+</sup> (CD8<sup>+</sup>) cells (Left), live IL-17A-producing CD4<sup>+</sup> and CD8<sup>+</sup> cells (CD4<sup>+</sup>IL-17A<sup>+</sup>, CD8<sup>+</sup>IL-17A<sup>+</sup>), live IFN- $\gamma$ -producing CD4<sup>+</sup> and CD8<sup>+</sup> cells (CD4<sup>+</sup>IFN- $\gamma$ <sup>+</sup> and CD8<sup>+</sup>IFN- $\gamma$ <sup>+</sup>) (Middle), and live IL-17A-producing  $\gamma\delta$ TCR<sup>low</sup> cells ( $\gamma\delta$ TCR<sup>low</sup>IL-17A<sup>+</sup>) (Right) in the ear pinnae. (B) Representative flow plots showing frequencies (mean  $\pm$  SEM) of IL-17A- or IFN- $\gamma$ -producing live CD4<sup>+</sup> in the ear pinnae of control SPF mice, *C. alb*-, *M. furfur*-, and *T. menta*-associated SPF mice. (C–F) SPF mice were topically associated with media (control) or various commensal fungi four times every other day. Fourteen days after the initial commensal association, mice were treated with IMQ cream 5 consecutive days or not (control). (C) (Top) Schematic of the treatment. (Bottom) Time course of percentage of ear thickness change relative to baseline at day 0 in the different groups of mice. (D) H&E staining of ear pinnae from control, *C. albicans*-associated (*C. alb*), IMQ-treated (IMQ), and *C. albicans*-associated and IMQ-treated (*C. alb*/IMQ) SPF mice. (Scale bar, 100  $\mu$ m.) (E) Frequencies (flow plots) and absolute numbers (graph) of live IL-17A- and/or IFN- $\gamma$ -producing CD4<sup>+</sup>Foxp3<sup>neg</sup> cells in the ear pinnae from control, IMQ-, *C. alb*-, and *C. alb*/IMQ SPF mice. (F) (Left) Representative flow plot showing the frequencies of live IL-17A- and ROR $\gamma$ t-expressing CD4<sup>+</sup>Foxp3<sup>neg</sup>CD44<sup>+</sup> T cells in ear pinnae of *C. albicans*/IMQ-treated SPF mice. (Right) Absolute numbers of ROR $\gamma$ t-expressing live CD4<sup>+</sup>Foxp3<sup>neg</sup>CD44<sup>+</sup> T cells (CD4<sup>+</sup>ROR $\gamma$ t<sup>+</sup>) in the ear pinnae from control (Ctrl), IMQ, *C. alb*, or *C. alb*/IMQ-treated SPF mice. (G) Time course of percentage of ear thickness change relative to baseline at day 0 after the start of IMQ treatment (Left) and absolute numbers (Right) of live IL-17A-producing CD45<sup>+</sup>CD90.2<sup>+</sup>TCR $\beta$ <sup>+</sup>CD4<sup>+</sup>Foxp3<sup>neg</sup> (CD4<sup>+</sup>IL-17A<sup>+</sup>) cells in the ear pinnae of unassociated SPF mice (IMQ) or in SPF mice previously associated with *C. albicans* 2 wk (*C. alb* 2W/IMQ), 1 mo (*C. alb* 1M/IMQ), or 2 mo (*C. alb* 2M/IMQ) prior to IMQ treatment. (H) Ear thickness (Left) and absolute numbers (Right) of live IL-17A-producing CD45<sup>+</sup>CD90.2<sup>+</sup>TCR $\beta$ <sup>+</sup>CD4<sup>+</sup>Foxp3<sup>neg</sup> (CD4<sup>+</sup>IL-17A<sup>+</sup>) cells in the ear pinnae of control germ-free mice (Ctrl), IMQ-, *C. alb*, and *C. alb*/IMQ germ-free mice. (I) Time course of percentage of ear thickness change relative to baseline at day 0 (Left) and absolute number (Right) of live IL-17A-producing CD45<sup>+</sup>CD90.2<sup>+</sup>TCR $\beta$ <sup>+</sup>CD4<sup>+</sup>Foxp3<sup>neg</sup> (CD4<sup>+</sup>IL-17A<sup>+</sup>) cells in the ear pinnae of SPF mice treated with IMQ or treated with IMQ after exposure to the standard strain of *C. albicans* (*C. alb*/IMQ), a yeast-locked strain of *C. albicans* (*hgc1* $\Delta$ /IMQ), or the control strain (*hgc1* $\Delta$ +HGC1<sup>+</sup>) for the yeast-locked *C. albicans* (HGC1+/IMQ). Cytokine production shown in this figure was analyzed following in vitro restimulation of the cells with PMA and ionomycin in the presence of brefeldin A. Results are representative of two to three independent experiments. \**P* < 0.05, \*\**P* < 0.01.

and leukocyte chemotaxis (Fig. 2B). We observed higher significance for all terms in the *C. albicans*/IMQ-treated sample as compared to IMQ alone. This analysis supports the idea that *C. albicans* association prior to IMQ enhanced tissue inflammation (compared to IMQ alone) but does not impact the overall transcriptional signature of the response.

To assess the potential relevance of our experimental approach to human psoriasis, we performed Ingenuity Pathway Analysis (IPA) disease term enrichment on genes differentially regulated in IMQ or *C. albicans*/IMQ-treated samples versus naïve control tissues. Notably, we found significant enrichment for dermatological diseases and conditions in both IMQ and *C. albicans*/IMQ-treated samples with *C. albicans*/IMQ showing a higher enrichment (Fig. 2C). Of note, psoriasis was the most activated term in dermatological diseases and conditions with *C.*

*albicans*/IMQ showing higher activation (Fig. 2D). This further confirmed that pretreatment with *C. albicans* exacerbates the inflammatory response without altering the quality of the response.

We next downloaded a list of 209 genes that were differentially expressed between lesional and uninvolved skin at the mRNA level and protein level in human patients with psoriasis (44) and overlaid these genes (153 up-regulated in lesional skin versus healthy skin, 56 down-regulated) with our list of mouse genes from whole tissue. This resulted in 177 shared genes. Gene clustering by similarity shows that *C. albicans*/IMQ-treated samples cluster closer and more robustly with samples from human skin lesion than whole-tissue mouse samples treated with IMQ alone (Fig. 2E). To further validate this finding, we downloaded RNA-seq data from 92 psoriatic and 82 normal human punch biopsies (45) and overlaid these data with our

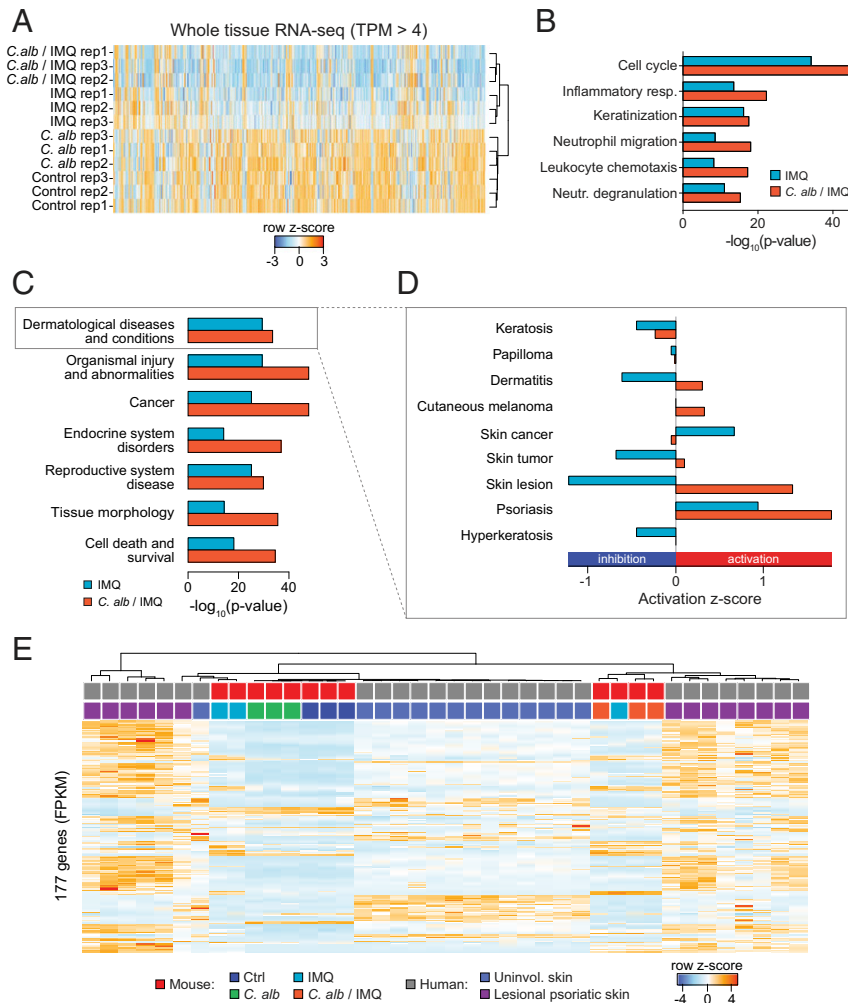


**Fig. 2.** Exposure to *C. albicans* prior to IMQ treatment provides a model more similar to human psoriatic lesional skin. (A) Heat map of whole-tissue gene expression for all genes with expression (TPM, transcripts per million) greater than 4 in all replicates in ear pinnae from control naïve SPF mice (control), *C. alb*-, IMQ-, and *C. alb*/IMQ-treated SPF mice. Colors depict row z-score. (B) GO annotation analysis for genes up-regulated in the ear pinnae of IMQ-treated SPF mice versus control naïve SPF mice (IMQ, blue) and genes up-regulated in the ear pinnae of *C. albicans*/IMQ-treated SPF mice versus control naïve SPF mice (*C. alb*/IMQ, orange). Up-regulated genes had fold change > 2, FDR < 5%. (C) Disease IPA analysis of whole-tissue RNA-seq for genes up-regulated in the ear pinnae from IMQ-treated SPF mice (blue) or from *C. alb*/IMQ-treated SPF mice (orange) in comparison to ear pinnae of control mice. (D) Zoom in view of disease terms in category "Dermatological Diseases and Conditions" for genes up-regulated in IMQ-treated versus control samples and up-regulated in *C. albicans*/IMQ (*C. alb*/IMQ)-treated versus control samples. Bars show z-score. Negative values show inhibition, whereas positive values show activation. (E) Clustering of 177 shared genes between differentially regulated genes in lesional psoriatic skin in mRNA and protein level in human patients versus unaffected skin (from the same patient) overlaid with mouse genes from whole-tissue RNA-seq from ear pinnae. Samples from human lesional psoriatic skin (purple) cluster closest with samples from *C. alb*/IMQ-treated SPF mice (orange), whereas samples from unaffected (uninvolved) human skin (blue) cluster closest with samples from IMQ-treated (IMQ) SPF mice (light blue), from control SPF mice (dark blue) and from *C. albicans*-treated (*C. alb*) SPF mice (green). Gene expression is normalized to fragments per kilobase per million (FPKM) and values are plotted as row z-score.

mouse samples, resulting in 2,658 common genes. Clustering the data by similarity of gene expression profile confirmed our previous analysis and showed a more robust clustering of *C. albicans*/IMQ-treated samples with human lesional psoriatic skin (SI Appendix, Fig. S2F).

Thus, exposure of mouse skin to *C. albicans* prior to IMQ treatment led to increased pathology associated with a tissue signature that closely recapitulates the transcriptional landscape of human lesional psoriatic skin.

**C. albicans-Associated Experimental Psoriasis Is Characterized by Enhanced Neutrophil Response and NET-Mediated Pathology.** Psoriatic lesions are characterized by neutrophil infiltrates, with spongiform pustules in the stratum spinosum and Munro's micro abscesses in the stratum corneum (46). In agreement with whole-tissue responses, preexposure to *C. albicans* in IMQ-treated mice significantly increased neutrophil infiltration compared to IMQ alone (Fig. 3A). A significant increase in inflammatory monocytes was also observed in tissue from *C. albicans*/IMQ treatment compared to *C. albicans* (SI Appendix, Fig. S3A). On the other hand, no differences were detected in the number of eosinophils, mast cells, or basophils compared to mice treated with IMQ alone (SI Appendix, Fig. S3B).

Enhanced activation of neutrophils in particular in the context of fungal exposure has been shown to be associated with the formation of neutrophil extracellular traps (NETs) (47, 48). NETosis is a defined process of cell death where neutrophils extrude DNA which extends into web-like threads (49). Electron microscopy imaging of *C. albicans*-exacerbated inflamed skin revealed web-like structures compatible with NETs at the surface of the epidermis in *C. albicans*/IMQ mice (Fig. 3B). To further confirm enhanced NETosis, we quantified histone H3 citrullination using confocal microscopy. NETosis is typically associated with activation of peptidylarginine deiminase 4 (PAD4)—a nuclear enzyme that is primarily expressed in neutrophils—which leads to histone H3 citrullination and chromatin decondensation (50). Imaging of whole ear pinnae revealed that IMQ (but not *C. albicans* alone) induced histone H3 citrullination (Fig. 3C). Notably, H3 citrullination was significantly increased in mice associated with *C. albicans* prior to IMQ treatment compared to IMQ alone (Fig. 3 C and D and SI Appendix, Fig. S3 C and D). These results support the idea that in the context of IMQ, previous skin colonization with a commensal fungus can promote aberrant neutrophil activation/death.

Enhanced NETs formation in the peripheral blood of psoriasis patients has been shown to correlate with psoriasis disease severity (51, 52). To test the possibility that enhanced NETosis may contribute to enhanced inflammation caused by *C. albicans* preexposure, mice were treated with DNase, an approach previously used to dismantle NETs (47). While DNase treatment had no significant impact on the pathogenesis of IMQ alone, this treatment significantly reduced inflammation induced by *C. albicans* prior to IMQ (Fig. 3E). Thus, exposure to fungi prior to IMQ can promote a feature of human psoriasis namely enhanced neutrophil activation and enhanced NETosis. These results support the idea that impacting NETs formation may have therapeutic value in defined psoriatic settings.

**Enhanced Pathology Induced by Preexposure to Skin Fungi Is Dectin-1/Langerhans Cell Dependent.** Previous work demonstrated that infection with the yeast form of *C. albicans* induced Th17 cell responses in a Langerhans cell (LC)-dependent manner (53, 54). Consistently, we found that Th17 responses following topical association with *C. albicans* were abolished in mice deficient in LCs (Lan-DTA) compared to wild-type control mice (Fig. 4A). In addition, *C. albicans* was no longer able to enhance the inflammation and neutrophil recruitment, as well as the accumulation of Th17 cells

induced by IMQ in mice deficient in LCs (Fig. 4 B, C, and F). In contrast *C. albicans* still promoted inflammation and cellular infiltrates in IMQ-treated mice lacking dermal dendritic cells (DCs) (*Batf3*<sup>-/-</sup> or *Irf4*<sup>fl/fl</sup> × *Igax*<sup>cre/+</sup>) (Fig. 4 C–F).

The fungi-responsive C-type lectin receptors (CLRs) play a central role in fungal detection during infection (55, 56). Notably, the CLR Dectin-1 (encoded by the *Clec7a* gene in mice) has been previously shown to recognize *C. albicans* yeast cells but not hyphae through binding to surface β-glucan (53). While *C. albicans* association did not alter the numbers and frequencies of the three main skin DC subsets (Fig. 4G), the intensity of Dectin-1 expression was significantly increased in LCs (but not in other DC subsets) from IMQ- and *C. albicans*/IMQ-treated mice (Fig. 4H). Further, enhanced inflammation associated with preexposure to *C. albicans* was abolished in mice deficient in Dectin-1 (*Clec7a*<sup>-/-</sup>) (Fig. 4I) and in mice deficient in the gene encoding its downstream adaptor molecule CARD9 (Fig. 4J). Thus, a Langerhans cell/Dectin-1 axis contributes to the enhanced Th17 cell responses and pathology associated with exposure to *C. albicans* prior to IMQ.

**C. albicans/IMQ Promotes Tissue Inflammation in a Candida-Specific Th17/Langerhans Cell-Dependent Manner.** In humans, lesional skin is characterized by a dominant accumulation of Th17 cells with limited numbers of γδ T cells (57). In contrast, in mice, IMQ-induced inflammation is associated with γδ T cell accumulation and tissue pathology, and is Vγ4<sup>+</sup>TCRγδ<sup>+</sup> cell dependent (58). In line with previous literature, γδ T cells were increased post-IMQ treatment (Fig. 5A). However, γδ T cells were not further increased by preexposure to *C. albicans* and enhanced pathology was still observed in Sox13-deficient mice [B6.SJL Cd45a(Ly5a)/Nai] that lack Vγ4<sup>+</sup>TCRγδ<sup>+</sup> cells (Fig. 5 A and B). This pointed to a dominant role for Th17 cells in enhanced pathology associated with fungal preexposure.

To address the role of Th17 in enhanced pathology caused by *C. albicans*, we utilized mice deficient in RORγt in αβ T cells (*Rorc*<sup>fl/fl</sup> × *Lck*<sup>cre/+/-</sup> mice). In these mice, and in contrast to controls, *C. albicans* did not enhance tissue inflammation (and neutrophil recruitment) provoked by IMQ (Fig. 5C). These results support the idea that in the context of fungal colonization, Th17 cells were the main mediator of enhanced pathology.

In order to gain better understanding of the status of activation of T cells induced by *C. albicans*/IMQ compared to T cells induced by *C. albicans* or IMQ alone, we sorted CD4<sup>+</sup> T cells (TCRβ<sup>+</sup>CD4<sup>+</sup>CD90.2<sup>+</sup>Foxp3<sup>neg</sup>) from the skin and performed RNA-seq in biological replicates (Fig. 5D). Samples clustered based on treatment (SI Appendix, Fig. S4 A and B) with *C. albicans*-treated samples as the outlier. Notably, 450 genes were differentially expressed between *C. albicans*- and *C. albicans*/IMQ-treated samples (FC > 2, FDR < 5%) (SI Appendix, Fig. S4C) and only 75 genes were differentially expressed between samples treated with IMQ versus *C. albicans*/IMQ (FC > 2, FDR < 5%) (SI Appendix, Fig. S4D). Functional analysis showed significant enrichment for genes involved in positive regulation of the MAPK cascade (a pathway also enriched in human psoriasis) (59), hematopoietic cell lineage, inflammation, and cytokine–cytokine receptor interaction (Fig. 5E) in *C. albicans*/IMQ samples compared to IMQ alone.

We next performed IPA to assess which pathways were activated and inhibited in the pairwise comparison of the different conditions (Fig. 5F). Confirming previous analysis, the p38 MAPK signaling pathway was activated in T cells from *C. albicans*/IMQ-treated mice (Fig. 5F). Further, and in agreement with our observations, the most activated pathway in *C. albicans*/IMQ versus all other conditions was the Th17 pathway with significant up-regulation of *Il17a*, *Il17f*, *Il22*, and down-regulation of *Il10* gene expression (Fig. 5 F and G). Notably, expression of genes

associated with T cell regulation/exhaustion was generally down-regulated in *C. albicans*/IMQ compared to IMQ alone (*SI Appendix, Fig. S4E*).

We next assessed if Th17 cells recruited to the skin of *C. albicans*/IMQ-treated mice were enriched in *C. albicans* specificities (as opposed to bystander). To this end, we purified Th17 (CD45<sup>+</sup>CD90.2<sup>+</sup>CD4<sup>+</sup>Foxp3<sup>neg</sup>CCR6<sup>+</sup>) cells from the regional lymph nodes (LNs) of mice preexposed to *C. albicans*/IMQ and cocultured them ex vivo with antigen-presenting cells (APCs) exposed to fungal antigens. Exposure of CD4<sup>+</sup>Foxp3<sup>neg</sup>CCR6<sup>+</sup> T cells to DCs loaded with *C. albicans*-derived antigens (heat-killed or *C. albicans*-conditioned medium) promoted IL-17A production supporting the idea that significant priming to *C. albicans*-derived antigens occurred under these settings (Fig. 5H). In vitro recall was abolished when DCs were deficient in major histocompatibility complex II (MHC-II) confirming that in our experimental settings, significant priming of *Candida*-specific T cells can be detected (Fig. 5H and *SI Appendix, Fig. S4F*). Of note, *C. albicans* association alone was also associated with the induction of IL-17-producing T cells within the regional LN but to a lower frequency than in mice associated with *C. albicans* prior to IMQ treatment (*SI Appendix, Fig. S4G*). Thus, these results support the idea that *C. albicans* association is sufficient to prime *C. albicans*-specific Th17 responses in a homeostatic way and that these responses can be amplified (and/or recalled) in the context of subsequent exposure to IMQ.

Altogether our results propose that recall responses to commensal skin fungi can significantly aggravate tissue inflammation.

In our model, enhanced pathology caused by fungal preexposure depends on Th17 responses and neutrophil extracellular traps (*SI Appendix, Fig. S5*) and recapitulates features of the transcriptional landscape of human lesional psoriatic skin.

## Discussion

Together, our results support the idea that adaptive immunity to skin fungi directly promotes skin inflammation and that pre-exposure to canonical commensal microbes can provide a model of experimental psoriasis with translational relevance. There is a growing appreciation that mouse models devoid of physiological microbial exposure may limit our ability to predict or model human homeostatic and disease settings (60–63). As such, development of mouse models that more closely reproduce human disease pathophysiology is of importance to our understanding of disease etiology and for the development of relevant preclinical models. In this context, we found that our experimental approach that takes into account preexposure to fungal microbiota allows a closer recapitulation of human psoriasis, namely, dependency on Th17 cells, enhanced neutrophils, keratinocyte activation, and NETs formation.

Our observation that fungal preexposure promotes IMQ pathology in a Th17-dependent manner as opposed to the traditional model that relies on  $\gamma\delta$  T cells is of particular relevance to human psoriasis that is dominated by Th17 but not  $\gamma\delta$  T cells (57). Further our model is in agreement with the known prevalence of fungal-specific type-17 immune responses in the human population (35). Of importance, fungi-specific Th17 cells have been

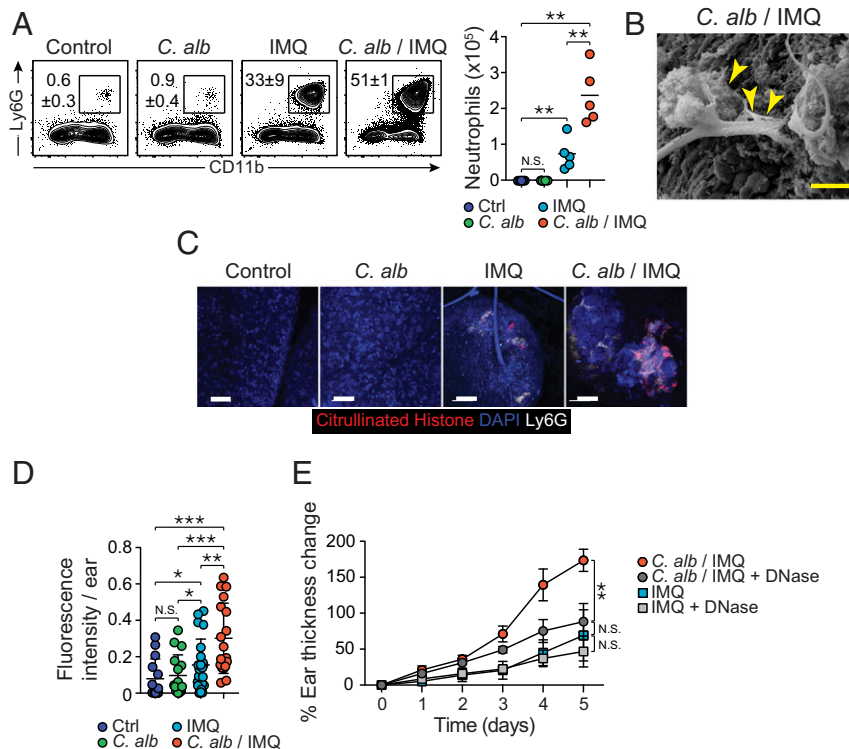


**Fig. 3.** Preexposure to *C. albicans* leads to enhanced neutrophil response and NETs-mediated pathology. (A) Representative flow plots showing frequencies of live neutrophils in the ear pinnae of naïve control (Ctrl), *C. alb*-, IMQ-, and *C. alb*/IMQ-treated SPF mice (Left). Absolute numbers of live neutrophils in the ear pinnae from the different groups of mice (Right). (B) Representative image of the surface of the ear pinnae from *C. albicans*/IMQ-treated SPF mouse obtained by scanning electron microscope. (Scale bar, 100  $\mu$ m.) Arrows indicate web-like structures on the surface of the ear. (C) Representative images of high magnification of whole mouse ear pinnae sections from untreated control SPF mice, *C. alb*-, IMQ-, and *C. alb*/IMQ-treated SPF mice showing DAPI (blue), citrullinated histone H3<sup>+</sup> cells (red), and Ly6G (white). (Scale bars, 50  $\mu$ m.) (D) NETs frequency evaluated by fluorescence intensity of citrullinated histone H3 per ear pinnae from untreated control (Ctrl) SPF mice, *C. alb*-, IMQ-, and *C. alb*/IMQ-treated SPF mice. (E) Time course of percentage of ear thickness change relative to baseline at day 0 from IMQ- and *C. alb*/IMQ-treated SPF mice and from IMQ- and *C. albicans*/IMQ-treated SPF mice following DNase treatment (IMQ + DNase and *C. alb*/IMQ + DNase). Results are representative of two to three independent experiments. \**P* < 0.05, \*\**P* < 0.01, \*\*\**P* < 0.001; N.S., not significant.

shown to cross-react to antigens expressed by diverse fungi and to expand in patients with airway inflammation (36). As such fungal immunity may underly numerous type-17-dependent inflammatory processes across barrier sites colonized by the microbiota.

While much remains to be done to confirm our hypothesis in the context of clinical settings, a link between fungal colonization and psoriasis has been previously proposed. For instances, a high rate of concomitant fungal infections was found in psoriatic nail patients (64, 65) and enhanced *Candida* colonization was associated with more severe disease states (28). Further, *Candida* species detection rates for psoriatic patients have been shown to be significantly higher than in healthy individuals (29), especially in the oral mucosa (33, 66, 67). These observations together with our present data support the idea that fungal colonization and/or infection at various sites including the oral mucosa may predispose to psoriasis or amplify this disorder via systemic enrichment of fungal reactive Th17 cells.

Our specific model associated with fungal preexposure recapitulated a role for NETs in the physiopathology of experimental psoriasis that was not detected in the model of IMQ alone. While NETs have been shown to contribute to the clearance of extracellular pathogens and in particular fungi (49), NETs are also enhanced in the skin and blood of psoriatic patients and disease severity has been associated with heightened NETs formation (51, 52). As such, previous work proposed that NETosis, via plasmacytoid dendritic cells activation, could directly promote psoriasis initiation and exacerbation (52, 68–70). Our experimental work further supports the idea that the Th17/NETs axis, a response that has evolved as a mean to primarily constrain fungal infections, may play an important role in the pathophysiology of psoriasis. As such, local DNase treatment may represent a potential therapeutic avenue in defined psoriatic settings.

Together our results also support the idea that exploration of tissue immunity and pathologies needs to take into account the

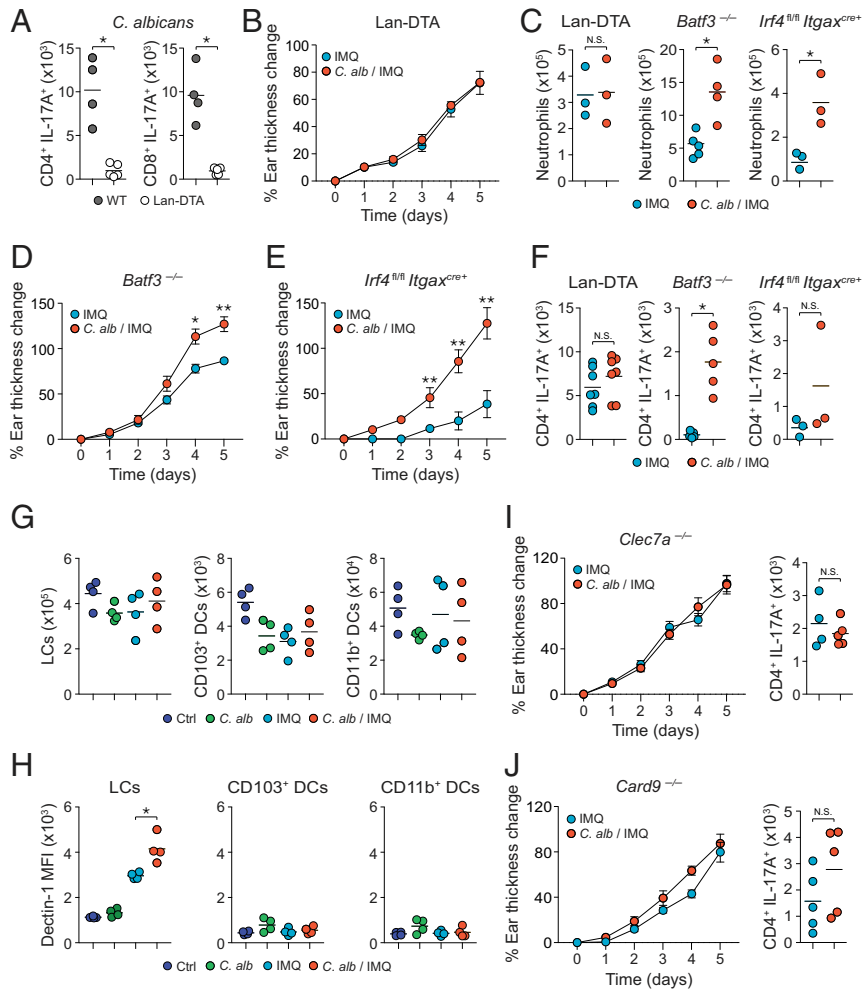


**Fig. 4.** Langerhans cells promote the commensal-derived immune responses. (A) Absolute number of live IL-17A-producing CD4<sup>+</sup>Foxp3<sup>neg</sup> T cells (CD4<sup>+</sup>IL-17A<sup>+</sup>) and IL-17A-producing CD8<sup>+</sup> T cells (CD8<sup>+</sup>IL-17A<sup>+</sup>) after *C. albicans* association in the ear pinnae from Lan-DTA and wild-type littermate control (WT) SPF mice. (B) Percentage of ear thickness change relative to baseline at day 0 from IMQ- and *C. albicans*/IMQ (*C. alb*/IMQ)-treated Lan-DTA SPF mice. (C) Absolute numbers of live neutrophils in the ear pinnae from IMQ- and *C. albicans*/IMQ (*C. alb*/IMQ)-treated Lan-DTA, *Batf3*<sup>-/-</sup>, and *Irf4*<sup>fl/fl</sup> *Itgax*<sup>cre/+</sup> SPF mice. (D and E) Percentage of ear thickness change relative to baseline at day 0 from IMQ- and *C. albicans*/IMQ (*C. alb*/IMQ)-treated *Batf3*<sup>-/-</sup> (D) and *Irf4*<sup>fl/fl</sup> *Itgax*<sup>cre/+</sup> (E) SPF mice. (F) Absolute numbers of live IL-17A-producing CD4<sup>+</sup>Foxp3<sup>neg</sup> (CD4<sup>+</sup>IL-17A<sup>+</sup>) T cells from the ear pinnae of IMQ- and *C. albicans*/IMQ (*C. alb*/IMQ)-treated Lan-DTA, *Batf3*<sup>-/-</sup>, and *Irf4*<sup>fl/fl</sup> *Itgax*<sup>cre/+</sup> SPF mice. (G) Absolute numbers of LCs, CD103<sup>+</sup> DCs, and CD11b<sup>+</sup> DCs in the ear pinnae from Ctrl, *C. alb*-, IMQ-, or *C. alb*/IMQ-treated SPF mice. (H) Dectin-1 mean fluorescence intensity (MFI) of DC subsets in the ear pinnae from Ctrl, *C. alb*-, IMQ-, or *C. alb*/IMQ-treated SPF mice. (I and J) Percentage of ear thickness change relative to baseline at day 0 (Left) and absolute numbers (Right) of live IL-17A-producing CD4<sup>+</sup>Foxp3<sup>neg</sup> (CD4<sup>+</sup>IL-17A<sup>+</sup>) T cells in the ear pinnae from IMQ- and *C. alb*/IMQ-treated *Clec7a*<sup>-/-</sup> (I) or *Card9*<sup>-/-</sup> (J) SPF mice. Cytokine production shown in this figure was analyzed following in vitro restimulation of the cells with PMA and ionomycin in the presence of brefeldin A. Results are representative of two to three independent experiments with the exception of results shown for Lan-DTA mice in F, which are a compilation of results from two independent experiments. \**P* < 0.05, \*\**P* < 0.01; N.S., not significant.

entwined relationship of the host with its microbiota and more particularly past and concomitant exposure to its resident microbes. Indeed, based on the large number of microbes colonizing all barrier surfaces, the majority of circulating and tissue resident memory/effector T cells are likely to be commensal specific. As such we could speculate that all inflammatory triggers that target microbiota-exposed tissues occur in the context of commensal-specific T cell recall responses. While our findings support the idea that fungal immunity may play an important role in tissue inflammation, we could propose that other canonical members of the skin microbiota able to promote type-17

responses could also contribute to this phenomenon. Development of tools allowing to track commensal-specific T cells in both experimental models and human tissues would allow further exploration of the contribution of commensal-specific immunity to disease etiology.

### Experimental Procedures

**Mice.** The following gender- and age-matched (6- to 16-wk-old) mice were used for experiments: specific pathogen free (SPF) and germ-free C57BL/6, B6.SJL Cd45a(Ly5a)/Nai (B6.SJL), C57BL/6NTac-[KO]Abb/B2m (*MHCII*<sup>-/-</sup>), B6.129P2(C)-*Baft3tm1Kmm/J* (*Batf3*<sup>-/-</sup>), B6.SJL-Cd45a(Ly5a)Nai-[KO]RAG1

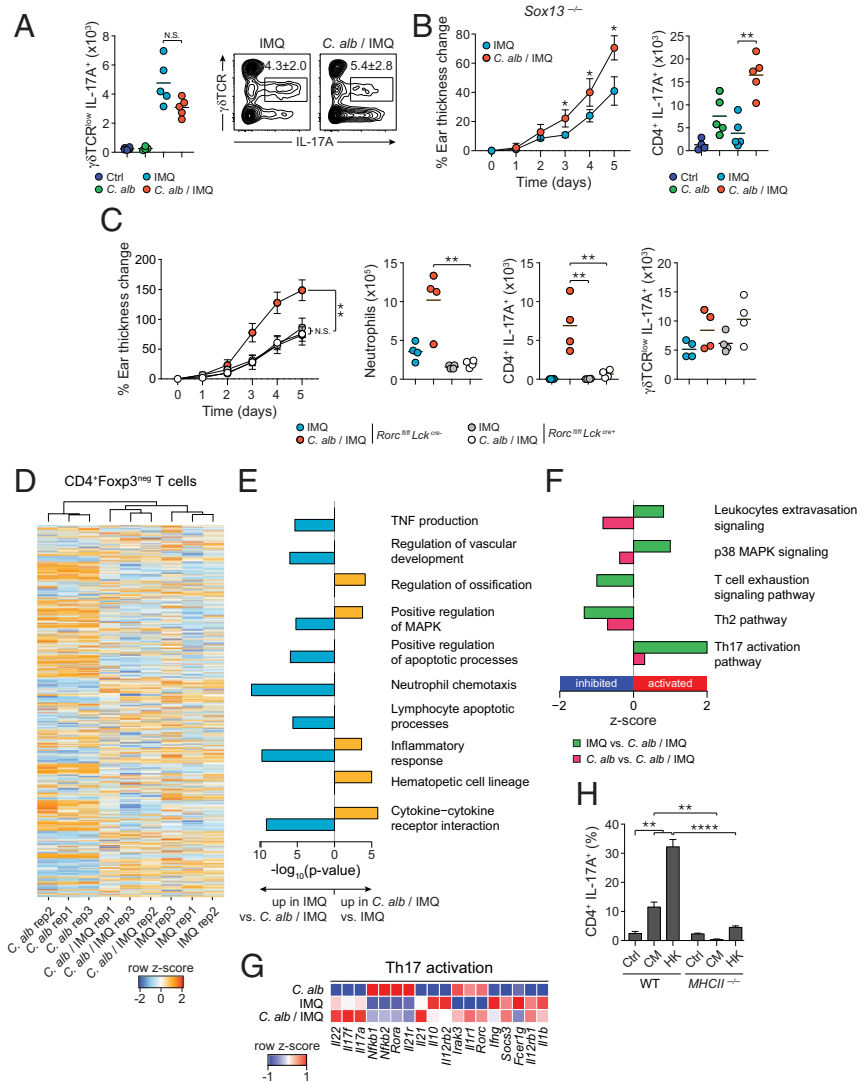


**Fig. 5.**  $\alpha\beta$ T cells but not  $\gamma\delta$ T cells promote the commensal-derived IL-17A immune responses. (A) Absolute numbers of live IL-17A-producing  $\gamma\delta\text{TCR}^{\text{low}}$  ( $\gamma\delta\text{TCR}^{\text{low}}\text{IL-17A}^+$ ) cells in the ear pinnae of Ctrl, C. alb-, IMQ-, or C. alb/IMQ-treated SPF mice (Left). Representative flow plots showing frequency of live IL-17A-producing  $\gamma\delta\text{TCR}^{\text{low}}$  cells in the ear pinnae of IMQ- and C. albicans/IMQ-treated mice (Right). (B) Percentage of ear thickness change relative to baseline at day 0 (Left) and absolute numbers of live IL-17A-producing  $\text{CD}4^+\text{Foxp}3^{\text{neg}}$  ( $\text{CD}4^+\text{IL-17A}^+$ ) T cells (Right) in the ear pinnae of IMQ- and C. alb/IMQ-treated B6.SJL-Cd45a(Ly5a)/Nai (*Sox13*<sup>-/-</sup>) SPF mice lacking  $\gamma\delta\text{TCR}^{\text{low}}\text{V}\gamma 4^+$  cells. (C) Percentage of ear thickness change relative to baseline at day 0 of IMQ- and C. alb/IMQ-treated *Lck*<sup>cre/+</sup>*Rorc*<sup>fl/fl</sup> SPF mice and *Lck*<sup>cre/+</sup>*Rorc*<sup>fl/fl</sup> SPF mice (Left). Absolute numbers of live neutrophils, IL-17A-producing  $\text{CD}4^+\text{Foxp}3^{\text{neg}}$  ( $\text{CD}4^+\text{IL-17A}^+$ ) T cells, and IL-17A-producing  $\gamma\delta\text{TCR}^{\text{low}}$  T cells in the ear pinnae (Right). (D) Heat map showing row z-score log normalized transcripts per million (TPM) for  $\text{TCR}\beta^+\text{CD}90.2^+\text{CD}4^+\text{Foxp}3^{\text{neg}}$  T cells from the ear pinnae of C. alb-, IMQ-, and C. alb/IMQ-treated SPF mice in replicates. (E) Gene ontology analysis for genes up-regulated in IMQ versus C. albicans/IMQ (Left side) and up-regulated in C. albicans/IMQ versus IMQ (Right side) in T cells from ear pinnae. (F) IPA pathway analysis for genes differentially regulated between T cells in the ear pinnae from IMQ versus C. alb/IMQ in green, and C. alb versus C. alb/IMQ in red. Positive bars show activation, whereas negative bars show inhibition. (G) Heat map showing row z-score of genes associated with Th17 activation from IPA analysis in F. (H)  $\text{CD}4^+\text{Foxp}3^{\text{neg}}\text{CCR}6^+$  T cells from the skin draining LNs of C. alb-, IMQ-, and C. alb/IMQ-treated SPF mice were cocultured with splenic dendritic cells derived from *Rag1*<sup>-/-</sup> (WT) or *MHCII*<sup>-/-</sup> untreated (Ctrl) or preincubated with C. albicans conditioned media (CM) or heat killed C. albicans (HK). Bar plot shows frequencies of  $\text{CD}4^+$  T cells expressing IL-17A in overnight cocultures. Cytokine production shown in this figure was analyzed following in vitro restimulation of the cells with PMA and ionomycin in the presence of brefeldin A. For A–C, and H results are representative of two to three independent experiments. \**P* < 0.05, \*\**P* < 0.01; \*\*\*\**P* < 0.0001; N.S., not significant.

(*Rag1*<sup>-/-</sup>), C57BL/6-[TgH]EGFP:Foxp3 (FoxP3-GFP reporter), B6.FVB-Tg(CD207-Dta)312Dhka/J (Lan-DTA), *Irf4*<sup>fl/fl</sup> × *Itgax*<sup>cre+</sup>, *Rorc*<sup>fl/fl</sup> × *Lck*<sup>cre+</sup>, B6.129S6-Card9tm1Xlin/J (*Card9*<sup>-/-</sup>) and B6.129S6-Clec7atm1Gdb/J (*Clec7a*<sup>-/-</sup>). All experiments were performed at the National Institute of Allergy and Infectious Diseases (NIAID) under an animal study proposal approved by the NIAID Animal Care and Use Committee.

**Imiquimod Induced Psoriasis-like Dermatitis.** Mice between 6 and 16 wk of age were treated daily for 5 consecutive days on each ear pinnae with 10 mg of 5% IMQ cream (Aldara Cream 5%; 3M Health Care). Ear thickness was measured before the first application, then daily during IMQ topical application and the day after the last topical application of IMQ with a digimatic caliper (Mitutoyo).

**Topical Association and Intra-dermal Infection of Mice with Fungi Species.** Unless stated otherwise, a strain isolated from the ear pinnae of *Il22*<sup>-/-</sup> mice was used for *C. albicans*. Other strains of fungi used were: the reference strain of *C. albicans* SC5314 (ATCC MYA-2876); a *C. albicans* strain isolated from human psoriatic skin (referred to as human *C. albicans*); a yeast-locked *C. albicans* (*hgc1Δ*) and its control strain *hgc1Δ*+HGC1<sup>+</sup>; *M. furfur* strain (ATCC 14521); and *T. mentagrophytes* strain (ATCC 18748). For topical association, mice were associated with fungi by applying fungal suspension (10<sup>9</sup> CFU/mL) using a sterile cotton swab. Application of fungal suspension was repeated every other day for 8 d. For intra-dermal infection, mice were injected with 10<sup>7</sup> CFU of *C. albicans*.

**DNase Treatment.** Mice were intraperitoneally injected daily with 1,000 IU of DNase I from bovine pancreas (Sigma-Aldrich) resuspended in phosphate buffered saline (PBS) starting 2 d prior to the imiquimod treatment and during the whole duration of the imiquimod treatment.

**Tissue Processing.** Mice were killed 14 d after the first topical application of *C. albicans* and/or the day after the last topical application of IMQ. Single-cell suspension from the skin draining lymph nodes or the ear pinnae were isolated as previously described (3).

**In Vitro Restimulation.** To analyze basal cytokine potential, single-cell suspensions from various tissues were cultured directly ex vivo in a 96-well U-bottom plate in RPMI 1640 media supplemented with 10% fetal bovine serum (FBS), 2 mM L-glutamine, 1 mM sodium pyruvate and nonessential amino acids, 20 mM Hepes, 100 U/mL penicillin, 100 μg/mL streptomycin, 50 μM β-mercaptoethanol and stimulated with 50 ng/mL phorbol myristate acetate (PMA) (Sigma-Aldrich) and 5 μg/mL ionomycin (Sigma-Aldrich) in the presence of brefeldin A (GolgiPlug, BD Biosciences) diluted per manufacturer's instructions for 2.5 h at 37 °C in 5% CO<sub>2</sub>. Following stimulation, cells were analyzed for intracellular cytokine production as described below.

**Flow Cytometry.** Single-cell suspensions were first stained with fluorochrome-conjugated antibodies against surface markers for 20 to 30 min at 4 °C in PBS and then washed twice with cold PBS. LIVE/DEAD Fixable Blue Dead Cell Stain Kit (Invitrogen Life Technologies) was used to exclude dead cells. For intracellular staining, cells were fixed/permeabilized for 30 min, washed twice, and then stained intracellularly for at least 1 h using the Foxp3/transcription factor staining buffer set (Life Technologies eBioscience) and fluorochrome-conjugated antibodies against cytokines and transcription factors. Each staining was performed in the presence of purified anti-mouse CD16/32 (clone 93) and 0.2 mg/mL purified rat gamma globulin (Jackson Immuno-research). Flow cytometric data were acquired on an LSR II or LSR Fortessa (BD Biosciences) and analyzed using FlowJo software (TreeStar).

**Histology.** Mice were killed 19 d after first topical application of *C. albicans* or the day after the last topical application of IMQ. The ear pinnae from each mouse were removed and fixed in PBS containing 10% formalin. Paraffin-embedded sections were cut at 0.5 mm, stained with hematoxylin and eosin (H&E), and examined histologically. PAS staining was performed on ear pinnae following 10% formalin fixation. Histological scoring was performed as reported previously (71). Briefly, inflammation, neutrophils, mononuclear

cells, edema, and epithelial hyperplasia were graded from 0 to 4 as follows: 0, no response; 1, minimal response; 2, mild response; 3, moderate response; and 4, marked response.

**Microscopy of Ear Pinnae.** Scanning microscopy of the surface of the ear pinnae was performed using a ZEISS Crossbeam 540 scanning electron microscope. Confocal microscopy was performed as previously described (37). Ear pinnae images were captured on a Leica M205 stereomicroscope and analyzed using Imaris Bitplane software.

**RNA-Seq Library Preparation.** Cells from ear pinnae were sorted on a BD FACS Aria (BD Biosciences). RNA was extracted using the Arcturus PicoPure RNA Isolation kit (Applied Biosystems) according to manufacturer's instructions. For T cell RNA-seq, the Clontech SMARTer Ultra Low mRNA library preparation kit was used and samples were sequenced paired end on an Illumina HiSeq 4000. For whole-tissue RNA-seq, the RNeasy Fibrous Tissue Mini Kit (Qiagen) was used and samples were sequenced single-end on an Illumina NextSeq 500.

**RNA-Seq Analysis.** RNA-seq samples were trimmed and subsequently mapped to the mm10 mouse genome with STAR (72) and quality control was performed with FastQC. Gene expression was assessed using HOMER's analyzeRepeats with parameters rna, mm10, -count exons, -condenseGenes (73). Raw data are shown as transcripts per million (TPM). Principal component analysis (PCA) was done with R. Differential expression was calculated using DESeq2 (74). Genes were considered differentially expressed with FDR < 0.05 and FC > 2. Gene ontology analysis was done with metascap (75) or IPA (Qiagen). To overlay mouse genes with human genes, RefSeq gene identifier was used. Mouse data were normalized the same way as the published human dataset (fragments per kilobase per million [FPKM] or reads per kilobase per million [RPKM]). The Gene Expression Omnibus (GEO) database accession nos. for the human datasets overlaid with our murine datasets are GSE67785 (Fig. 2E) and GSE54456 (SI Appendix, Fig. S2F).

**Dendritic Cell and T-Cell Coculture Assay.** Purified CD4<sup>+</sup> (CD45<sup>+</sup>CD90.2<sup>+</sup>CD4<sup>+</sup>Foxp3<sup>neg</sup>CCR6<sup>+</sup>) T cells were cocultured for 16 h at 37 °C in 5% CO<sub>2</sub> with splenic CD11c<sup>+</sup> dendritic cells left untreated or previously incubated with or without heat-killed *C. albicans* (*C. albicans*:SpDC ratio, 500:1) or *C. albicans*-conditioned medium. Brefeldin A (GolgiPlug) was added for the final 90 min of the culture.

**Statistics.** Data are presented as mean (scatterplots) or mean ± SEM (ear thickness plots). Statistical significance was determined with the two-tailed unpaired Student's *t* test, under the untested assumption of normality. Bar graphs show mean of several datapoints and significance was assessed using a one-way ANOVA with multiple comparisons. All statistical analyses were calculated using Prism software (GraphPad). Differences were considered to be statistically significant when *P* < 0.05.

**Data Availability.** The RNA-seq datasets were deposited with NCBI under accession no. GSE144850. A full overview of the methods can be found in SI Appendix.

**ACKNOWLEDGMENTS.** This work was supported by NIAID Division of Intramural Research (#Projects ZIA-AI001115, ZIA-AI001132) (Y.B.), (Project ZIA-AI001175) (M.S.L.); National Institute of Arthritis and Musculoskeletal and Skin Diseases Division of Intramural Research (Project ZIA-AR041199) (M.J.K.); Collège des Enseignants de Dermatologie Français, Société Française de Dermatologie, Philippe Foundation, Fondation La Roche Posay, and Fondation pour la Recherche Médicale (C.H.); European Molecular Biology Organization (Fellowship ALTF 1535-2014) and Fondation ARC pour la Recherche sur le Cancer (S.T.); Japan Society for the Promotion of Science Fellowship for Japanese Biomedical and Behavioral Researchers at NIH (S.N.). We thank the NIAID animal facility staff; K. Holmes, E. Stregevsy, and T. Hawley (NIAID Flow Cytometry Facility); and E. Lewis and K. Beacht for technical assistance. We acknowledge the NIAID Microbiome Program gnotobiotic animal facility for experiments using germ-free mice. This study used the Office of Cyber Infrastructure and Computational Biology High Performance Computing cluster at NIAID.

1. Y. Belkaid, O. J. Harrison, Homeostatic immunity and the microbiota. *Immunity* **46**, 562–576 (2017).
2. Y. Cong, T. Feng, K. Fujihashi, T. R. Schoeb, C. O. Elson, A dominant, coordinated T regulatory cell-gA response to the intestinal microbiota. *Proc. Natl. Acad. Sci. U.S.A.* **106**, 19256–19261 (2009).

3. S. Naik et al., Compartmentalized control of skin immunity by resident commensals. *Science* **337**, 1115–1119 (2012).
4. Y. Yang et al., Focused specificity of intestinal TH17 cells towards commensal bacterial antigens. *Nature* **510**, 152–156 (2014).

5. J. L. Linehan *et al.*, Non-classical immunity controls microbiota impact on skin immunity and tissue repair. *Cell* **172**, 784–796.e18 (2018).
6. A. N. Hegazy *et al.*, Interferons direct Th2 cell reprogramming to generate a stable GATA-3(+)/T-bet(+) cell subset with combined Th2 and Th1 cell functions. *Immunity* **32**, 116–128 (2010).
7. T. W. Hand *et al.*, Acute gastrointestinal infection induces long-lived microbiota-specific T cell responses. *Science* **337**, 1553–1556 (2012).
8. S. Preite *et al.*, Hyperactivated PI3K $\delta$  promotes self and commensal reactivity at the expense of optimal humoral immunity. *Nat. Immunol.* **19**, 986–1000 (2018).
9. H. J. Wu *et al.*, Gut-residing segmented filamentous bacteria drive autoimmune arthritis via T helper 17 cells. *Immunity* **32**, 815–827 (2010).
10. K. Honda, D. R. Littman, The microbiota in adaptive immune homeostasis and disease. *Nature* **535**, 75–84 (2016).
11. Y. E. Chen, M. A. Fischbach, Y. Belkaid, Skin microbiota-host interactions. *Nature* **553**, 427–436 (2018).
12. Y. Belkaid, J. A. Segre, Dialogue between skin microbiota and immunity. *Science* **346**, 954–959 (2014).
13. R. L. Gallo, Human skin is the largest epithelial surface for interaction with microbes. *J. Invest. Dermatol.* **137**, 1213–1214 (2017).
14. S. L. Gaffen, R. Jain, A. V. Garg, D. J. Cua, The IL-23-IL-17 immune axis: From mechanisms to therapeutic testing. *Nat. Rev. Immunol.* **14**, 585–600 (2014).
15. D. A. Martin *et al.*, The emerging role of IL-17 in the pathogenesis of psoriasis: Pre-clinical and clinical findings. *J. Invest. Dermatol.* **133**, 17–26 (2013).
16. R. Speckaert *et al.*, The many faces of interleukin-17 in inflammatory skin diseases. *Br. J. Dermatol.* **175**, 892–901 (2016).
17. A. Fahlén, L. Engstrand, B. S. Baker, A. Powles, L. Fry, Comparison of bacterial microbiota in skin biopsies from normal and psoriatic skin. *Arch. Dermatol. Res.* **304**, 15–22 (2012).
18. Z. Gao, C. H. Tseng, B. E. Strober, Z. Pei, M. J. Blaser, Substantial alterations of the cutaneous bacterial biota in psoriatic lesions. *PLoS One* **3**, e2719 (2008).
19. A. V. Alekseyenko *et al.*, Community differentiation of the cutaneous microbiota in psoriasis. *Microbiome* **1**, 31 (2013).
20. Z. Zákostelská *et al.*, Intestinal microbiota promotes psoriasis-like skin inflammation by enhancing Th17 response. *PLoS One* **11**, e0159539 (2016).
21. P. Zanvit *et al.*, Antibiotics in neonatal life increase murine susceptibility to experimental psoriasis. *Nat. Commun.* **6**, 8424 (2015).
22. J. C. Arthur, C. Jobin, The struggle within: Microbial influences on colorectal cancer. *Inflamm. Bowel Dis.* **17**, 396–409 (2011).
23. N. Hernández-Santos, S. L. Gaffen, Th17 cells in immunity to *Candida albicans*. *Cell Host Microbe* **11**, 425–435 (2012).
24. J.-H. Jo, E. A. Kennedy, H. H. Kong, Topographical and physiological differences of the skin mycobiome in health and disease. *Virulence* **8**, 324–333 (2017).
25. K. Findley *et al.*, NIH Intramural Sequencing Center Comparative Sequencing Program, Topographic diversity of fungal and bacterial communities in human skin. *Nature* **498**, 367–370 (2013).
26. X. V. Li, I. Leonardi, I. D. Iliiev, Gut mycobiota in immunity and inflammatory disease. *Immunity* **50**, 1365–1379 (2019).
27. A. Takemoto, O. Cho, Y. Morohoshi, T. Sugita, M. Muto, Molecular characterization of the skin fungal microbiome in patients with psoriasis. *J. Dermatol.* **42**, 166–170 (2015).
28. N. Ovcina-Kurtović, E. Kasumagić-Halilović, H. Helppikangas, J. Begić, Prevalence of *Candida* species in patients with psoriasis. *Acta Dermatovenerol. Croat.* **24**, 209–213 (2016).
29. M. Taheri Sarvtin, T. Shokohi, Z. Hajheydari, J. Yazdani, M. T. Hedayati, Evaluation of candidal colonization and specific humoral responses against *Candida albicans* in patients with psoriasis. *Int. J. Dermatol.* **53**, e555–e560 (2014).
30. A. A. Bedair, A. M. Darwazah, M. M. Al-Aboosi, Oral *Candida* colonization and candidiasis in patients with psoriasis. *Oral Surg. Oral Med. Oral Pathol. Oral Radiol.* **114**, 610–615 (2012).
31. A. Waldman, A. Gilhar, L. Duek, I. Berdicevsky, Incidence of *Candida* in psoriasis—A study on the fungal flora of psoriatic patients. *Mycoses* **44**, 77–81 (2001).
32. B. L. Picciani *et al.*, Oral candidiasis in patients with psoriasis: Correlation of oral examination and cytopathological evaluation with psoriasis disease severity and treatment. *J. Am. Acad. Dermatol.* **68**, 986–991 (2013).
33. A. Pietrzak *et al.*, Prevalence and possible role of *Candida* species in patients with psoriasis: A systematic review and meta-analysis. *Mediators Inflamm.* **2018**, 9602362 (2018).
34. N. Crutcher *et al.*, Oral nystatin in the treatment of psoriasis. *Arch. Dermatol.* **120**, 435–436 (1984).
35. C. E. Zielinski *et al.*, Pathogen-induced human TH17 cells produce IFN- $\gamma$  or IL-10 and are regulated by IL-1 $\beta$ . *Nature* **484**, 514–518 (2012).
36. P. Bacher *et al.*, Human anti-fungal Th17 immunity and pathology rely on cross-reactivity against *Candida albicans*. *Cell* **176**, 1340–1355.e15 (2019).
37. S. Naik *et al.*, Commensal-dendritic-cell interaction specifies a unique protective skin immune signature. *Nature* **520**, 104–108 (2015).
38. P. Zwicky, S. Unger, B. Becher, Targeting interleukin-17 in chronic inflammatory disease: A clinical perspective. *J. Exp. Med.* **217**, e20191123 (2019).
39. L. van der Fits *et al.*, Imiquimod-induced psoriasis-like skin inflammation in mice is mediated via the IL-23/IL-17 axis. *J. Immunol.* **182**, 5836–5845 (2009).
40. K. Bocheńska, E. Smolińska, M. Moskot, J. Jakóbkiewicz-Banecka, M. Gabig-Cimińska, Models in the research process of psoriasis. *Int. J. Mol. Sci.* **18**, E2514 (2017).
41. R. R. Roth, W. D. James, Microbial ecology of the skin. *Annu. Rev. Microbiol.* **42**, 441–464 (1988).
42. N. A. R. Gow, F. L. van de Veerdonk, A. J. P. Brown, M. G. Netea, *Candida albicans* morphogenesis and host defence: Discriminating invasion from colonization. *Nat. Rev. Microbiol.* **10**, 112–122 (2011).
43. X. Zheng, Y. Wang, Y. Wang, Hgc1, a novel hypha-specific G1 cyclin-related protein regulates *Candida albicans* hyphal morphogenesis. *EMBO J.* **23**, 1845–1856 (2004).
44. W. R. Swindell *et al.*, Modulation of epidermal transcription circuits in psoriasis: New links between inflammation and hyperproliferation. *PLoS One* **8**, e79253 (2013).
45. B. Li *et al.*, Transcriptome analysis of psoriasis in a large case-control sample: RNA-seq provides insights into disease mechanisms. *J. Invest. Dermatol.* **134**, 1828–1838 (2014).
46. M. Schön, D. Denzer, R. C. Kubitzka, T. Ruzicka, M. P. Schön, Critical role of neutrophils for the generation of psoriasisiform skin lesions in flaky skin mice. *J. Invest. Dermatol.* **114**, 976–983 (2000).
47. V. Brinkmann *et al.*, Neutrophil extracellular traps kill bacteria. *Science* **303**, 1532–1535 (2004).
48. C. F. Urban, U. Reichard, V. Brinkmann, A. Zychlinsky, Neutrophil extracellular traps capture and kill *Candida albicans* yeast and hyphal forms. *Cell. Microbiol.* **8**, 668–676 (2006).
49. V. Papayannopoulos, Neutrophil extracellular traps in immunity and disease. *Nat. Rev. Immunol.* **18**, 134–147 (2017).
50. Y. Wang *et al.*, Human PAD4 regulates histone arginine methylation levels via demethyliminium. *Science* **306**, 279–283 (2004).
51. S. C. Hu *et al.*, Neutrophil extracellular trap formation is increased in psoriasis and induces human  $\beta$ -defensin-2 production in epidermal keratinocytes. *Sci. Rep.* **6**, 31119 (2016).
52. A. M. Lin *et al.*, Mast cells and neutrophils release IL-17 through extracellular trap formation in psoriasis. *J. Immunol.* **187**, 490–500 (2011).
53. S. W. Kashem *et al.*, *Candida albicans* morphology and dendritic cell subsets determine T helper cell differentiation. *Immunity* **42**, 356–366 (2015).
54. D. H. Kaplan, M. C. Jenison, S. Saeland, W. D. Shlomchik, M. J. Shlomchik, Epidermal langerhans cell-deficient mice develop enhanced contact hypersensitivity. *Immunity* **23**, 611–620 (2005).
55. M. J. Marakalala *et al.*, Differential adaptation of *Candida albicans* in vivo modulates immune recognition by dectin-1. *PLoS Pathog.* **9**, e1003315 (2013).
56. P. R. Taylor *et al.*, Dectin-1 is required for beta-glucan recognition and control of fungal infection. *Nat. Immunol.* **8**, 31–38 (2007).
57. T. R. Matos *et al.*, Clinically resolved psoriatic lesions contain psoriasis-specific IL-17-producing  $\alpha\beta$  T cell clones. *J. Clin. Invest.* **127**, 4031–4041 (2017).
58. E. E. Gray *et al.*, Deficiency in IL-17-committed V $\gamma$ 4(+)  $\gamma\delta$  T cells in a spontaneous Sox13-mutant CD45.1(+) congenic mouse substrain provides protection from dermatitis. *Nat. Immunol.* **14**, 584–592 (2013).
59. C. Johansen *et al.*, The mitogen-activated protein kinases p38 and ERK1/2 are increased in lesional psoriatic skin. *Br. J. Dermatol.* **152**, 37–42 (2005).
60. S. P. Rosshart *et al.*, Laboratory mice born to wild mice have natural microbiota and model human immune responses. *Science* **365**, eaaw4361 (2019).
61. L. K. Beura *et al.*, Normalizing the environment recapitulates adult human immune traits in laboratory mice. *Nature* **532**, 512–516 (2016).
62. S. P. Rosshart *et al.*, Wild mouse gut microbiota promotes host fitness and improves disease resistance. *Cell* **171**, 1015–1028.e13 (2017).
63. T. A. Reese *et al.*, Sequential infection with common pathogens promotes human-like immune gene expression and altered vaccine response. *Cell Host Microbe* **19**, 713–719 (2016).
64. S. Chaowattananapanit *et al.*, Coexistence of fungal infections in psoriatic nails and their correlation with severity of nail psoriasis. *Indian Dermatol. Online J.* **9**, 314–317 (2018).
65. A. Tsentemidou, T. A. Vyzantiadis, A. Kyriakou, D. Sotiriadis, A. Patsatsi, Prevalence of onychomycosis among patients with nail psoriasis who are not receiving immunosuppressive agents: Results of a pilot study. *Mycoses* **60**, 830–835 (2017).
66. S. Lesan *et al.*, Oral *Candida* colonization and plaque type psoriasis: Is there any relationship? *J. Investig. Clin. Dent.* **9**, e12335 (2018).
67. L. Chularojanamontri *et al.*, Oral *Candida* colonization in Thai patients with psoriasis. *J. Med. Assoc. Thai.* **99**, 84–87 (2016).
68. R. Lande *et al.*, Plasmacytoid dendritic cells sense self-DNA coupled with antimicrobial peptide. *Nature* **449**, 564–569 (2007).
69. J. M. Kahlenberg, M. J. Kaplan, Little peptide, big effects: The role of LL-37 in inflammation and autoimmune disease. *J. Immunol.* **191**, 4895–4901 (2013).
70. J. Skrzeczynska-Moncznik *et al.*, Secretory leukocyte proteinase inhibitor-competent DNA deposits are potent stimulators of plasmacytoid dendritic cells: Implication for psoriasis. *J. Immunol.* **189**, 1611–1617 (2012).
71. S. Nakajima *et al.*, Prostaglandin I2-IP signaling promotes Th1 differentiation in a mouse model of contact hypersensitivity. *J. Immunol.* **184**, 5595–5603 (2010).
72. A. Dobin *et al.*, STAR: Ultrafast universal RNA-seq aligner. *Bioinformatics* **29**, 15–21 (2013).
73. S. Heinz *et al.*, Simple combinations of lineage-determining transcription factors prime cis-regulatory elements required for macrophage and B cell identities. *Mol. Cell* **38**, 576–589 (2010).
74. M. I. Love, W. Huber, S. Anders, Moderated estimation of fold change and dispersion for RNA-seq data with DESeq2. *Genome Biol.* **15**, 550 (2014).
75. Y. Zhou *et al.*, Metascape provides a biologist-oriented resource for the analysis of systems-level datasets. *Nat. Commun.* **10**, 1523 (2019).